Solid State Sciences 13 (2011) 1291–1298

Contents lists available at ScienceDirect

Solid State Sciences

journal homepage: www.elsevier.com/locate/ssscie

The first principles study on the TmSb compound

C. Çoban [a,*], K. Çolakoğlu [b], Y.Ö. Çiftçi [b]

[a] Balıkesir University, Department of Physics, Çağış Campus, 10145 Balıkesir, Turkey
[b] Gazi University, Department of Physics, Teknikokullar, 06500 Ankara, Turkey

ARTICLE INFO

Article history:
Received 28 October 2010
Received in revised form
3 March 2011
Accepted 29 March 2011
Available online 3 April 2011

Keywords:
TmSb
Elastic properties
Thermodynamic properties
Lattice dynamics

ABSTRACT

The structural, elastic, electronic, thermodynamic, and phonon properties of TmSb which crystallizes in NaCl (B1) phase were analyzed by performing ab-initio calculations based on density functional theory using the Vienna Ab-initio Simulation Package (VASP). The exchange correlation potential within the generalized-gradient approximation (GGA) of Perdew–Burke–Ernzerhof (PBE) was used. The calculated structural parameters, such as the lattice constant, bulk modulus and its pressure derivative, cohesive energy, and second-order elastic constants are presented for B1 and CsCl (B2). This compound exhibits crystallographic phase transition from the B1 to B2 structure at pressure 29.13 GPa. In order to gain further information, for B1 phase, we investigated the elastic properties such as, Zener anisotropy factor, Poisson's ratio, Young's modulus, and shear modulus; the thermodynamic properties such as, the pressure and temperature dependent behavior of the normalized volume, bulk modulus, heat capacity, thermal expansion coefficient, Debye temperature, Grüneisen parameter, and entropy over a pressure range of 0–18 GPa and a temperature range of 0–1000 K. The electronic band structure, total density of states, phonon dispersion curves and one-phonon density of states of B1 phase are also presented. The obtained results are compared with the available experimental and theoretical data.

© 2011 Elsevier Masson SAS. All rights reserved.

1. Introduction

Rare-earth compounds have attracted experimental [1–14] and theoretical attention [15–23] because of the presence of strongly correlated f-electrons in them. They possess unusual and interesting structural, mechanical, and electronic properties which make them important materials for industrial and technological applications.

The pressure induced phase transitions in Thulium antimonide (TmSb) and other lanthanide monoantimonides with NaCl (B1) type structure have been studied experimentally by use of synchrotron radiation and the powder X-ray diffraction (XRD) by Shirotani et al. [24]. Their study on TmSb compound shows that this compound undergoes a pressure induced structural transformation from B1 to CsCl (B2) structure at 31 GPa. Abdusalyamova et al. [25] have measured the lattice parameter by X-ray method, measured thermal expansion coefficient in cylindrical specimens, and calculated Debye temperature of TmSb. Ott et al. [26] have reported a crystal-electric-field effect on the low-temperature thermal expansion of this compound. Y. H. Wong [27] has done low-temperature measurements on the electrical resistivity and thermal conductivity of pnictide compounds LSb (L = Er, Tm, La). The experimental results for the susceptibility and high-field anisotropic magnetization of TmSb have been presented by Cooper et al. [28]. Some elastic and thermodynamic measurements have been conducted on some rare-earth antimonides including the TmSb by Mullen et al. [29]. Hulliger et al. [30] have calculated the lattice parameters of all lanthanide monopnictides. The structural,elastic and thermal properties of three heavy mono-antimonides of holmium, erbium and thulium(LnSb, Ln = Ho, Er and Tm) have been investigated theoretically by using an interionic potential theory consisting of long-range Coulomb, short-range repulsive and van der Waal's (vdW) interactions by Soni et al. [31].

Here, we presented the structural, elastic, electronic, thermodynamic, and phonon properties of TmSb (Tm:0, 0, 0; Sb:1/2, 1/2, 1/2; space group $Fm\bar{3}m(225)$) using Vienna Ab-initio Simulation Package (VASP). The TmSb compound is reported to undergo a structural phase transition from an ambient B1 to high pressure B2 structure. The article is organized as follows. The calculation method is explained in Section 2. In Section 3, we presented our results and the comparison with the available experimental and other theoretical studies. Finally, conclusions are presented in Section 4.

2. Method of calculation

The present calculations are based on the first principles pseudo-potential method within the density functional formalism

* Corresponding author. Tel.: +90 266 6121278/1206; fax: +90 266 6121215.
E-mail addresses: cansucoban@yahoo.com (C. Çoban), kcolak@gazi.edu.tr (K. Çolakoğlu), yasemin@gazi.edu.tr (Y.Ö. Çiftçi).

1293-2558/$ – see front matter © 2011 Elsevier Masson SAS. All rights reserved.
doi:10.1016/j.solidstatesciences.2011.03.024

which were done by the Vienna Ab-initio Simulation Package (VASP) [32–36]. It performs an iterative solution of the generalized Kohn–Sham equations of density-functional theory, based on the minimization of the norm of the residual vector to each eigenstate and an efficient charge density mixing [37]. The exchange and correlation functional were treated by the generalized-gradient approximation (GGA) of Perdew–Burke–Ernzerhof (PBE) as proposed by Perdew, Burke, and Ernzerhof [38]. The projector-augmented wave (PAW) method developed by Blöchl [39] implemented within VASP was used to describe the interactions between ions and electrons. For the structure calculations, a plane-wave basis set with energy cut-off 500 eV was used. For the Brillouin zone sampling, the k-points of 12 × 12 × 12 were generated by using Monkhorst and Pack scheme [40].

The thermodynamic properties of TmSb compound were calculated by GIBBS program [41]. The GIBBS code is used to investigate isothermal-isobaric thermodynamics of a compound from energy curves using a quasi-harmonic Debye model. The non-equilibrium Gibbs function $G^*(V; P, T)$ within this model is defined as [42].

$$G^*(V;P,T) = E(V) + PV + A_{vib}[\Theta(V);T], \tag{1}$$

where $E(V)$ is the total energy for per unit cell of TmSb, PV is the constant hydrostatic pressure condition, $\Theta(V)$ is the Debye temperature and A_{vib} is the vibrational Helmholtz free energy which is given below [43–47]

$$A_{vib}(\Theta;T) = nkT\left[\frac{9\Theta}{8T} + 3\ln\left(1 - e^{-\Theta/T}\right) - D(\Theta/T)\right], \tag{2}$$

where n is the number of atoms per formula unit, $D(\Theta/T)$ represents the Debye integral. Θ is expressed as [45]

$$\Theta = \frac{\hbar}{k}\left[6\pi^2 V^{1/2} n\right]^{1/3} f(\sigma)\sqrt{\frac{B_S}{M}}, \tag{3}$$

where M is the molecular mass per unit cell and B_S is the adiabatic bulk modulus [41]. $f(\sigma)$ is taken from the Refs. [45,46], where σ is Poisson's ratio. Thus, the non-equilibrium Gibbs function $G^*(V; P, T)$ as a function of $(V; P, T)$ can be minimized with respect to V as in following equation

$$\left[\frac{\partial G^*(V;P,T)}{\partial V}\right]_{P,T} = 0. \tag{4}$$

The thermal equation of state (EOS) can be obtained by solving the Eq. (4). The entropy S, heat capacity at constant volume C_V, isothermal bulk modulus B_T, Grüneisen parameter γ, and thermal expansion coefficient α, of the system are given as in Eqs. (5–9) [41]

$$S = nk\left[4D(\Theta/T) - 3\ln\left(1 - e^{-\Theta/T}\right)\right], \tag{5}$$

$$C_V = 3nk\left[4D(\Theta/T) - \frac{3\Theta/T}{e^{\theta/T} - 1}\right], \tag{6}$$

$$B_T(P,T) = V\left(\frac{\partial^2 G^*(V;P,T)}{\partial V^2}\right)_{P,T}, \tag{7}$$

$$\gamma = -\frac{d\ln\Theta(V)}{d\ln V}, \tag{8}$$

$$\alpha = \frac{\gamma C_V}{B_T V}. \tag{9}$$

The present GGA_PBE phonon frequencies for TmSb compound in B1 phase were calculated by the PHON code [48] using the Helmann–Feynman forces obtained from the VASP. It calculates phonon frequencies and one-phonon density of states (DOS) generating all force constant matrix elements using the "Small Displacement Method" described in Ref. [49] which is a similar procedure as described in Ref. [50].

3. Results and discussion

3.1. Structural properties

The total energy as a function of volume curves were obtained by calculating the total energy at several different volumes and by fitting the calculated values to the Murnaghan equation of state [51] for each phase. The total energy versus volume (E–V) curves for the B1 and B2 phases of TmSb are shown in Fig. 1. The bulk properties such as lattice constant (a), bulk modulus (B), and pressure derivative of bulk modulus (B') are given in Table 1 along with the previous experimental and theoretical results. Optimized lattice constant is found to be 6.1354 Å for B1 structure and it agrees well with corresponding previous experimental values of 6.1054 and 6.08 Å taken from the Refs. [25] and [30], respectively. The lattice constant of B2 phase is found as 3.7643 Å. It is roughly 8.8% higher than the experimental data reported in Ref. [24]. The bulk modulus is calculated to be 60.71 GPa for B1 phase which is 15.4% and 13.32% lower than the experimental and theoretical values given in Refs. [29] and [31], respectively. Besides, the calculated pressure derivative of bulk modulus is 31.23% lower than the previous theoretical data [31].

To obtain the phase transition pressure (P_t) at zero temperature, generally, two methods are used: The first one is the calculation of enthalpy (H) and the second one is the calculation of the slope of E–V curves in Fig. 1 which is called "common tangent technique". We found from our investigations the TmSb compound undergoes a phase transition from B1 to B2 structure at high pressures. The variation of the enthalpy, H, for TmSb in both structures as a function of pressure (P)is shown in Fig. 2. The transition pressure, P_t, is a pressure at which the enthalpies of both B1 and B2 structures are the same which is determined by calculating the Gibb's free energies at 0 K. From Fig. 2, the transition pressure, P_t, from B1 to B2 structure is found to be 29.13 GPa. The same result is also confirmed in terms of the "common tangent technique" in Fig. 1 (about 29.38 GPa from Fig. 1). These results are slightly (about 5–6%) lower

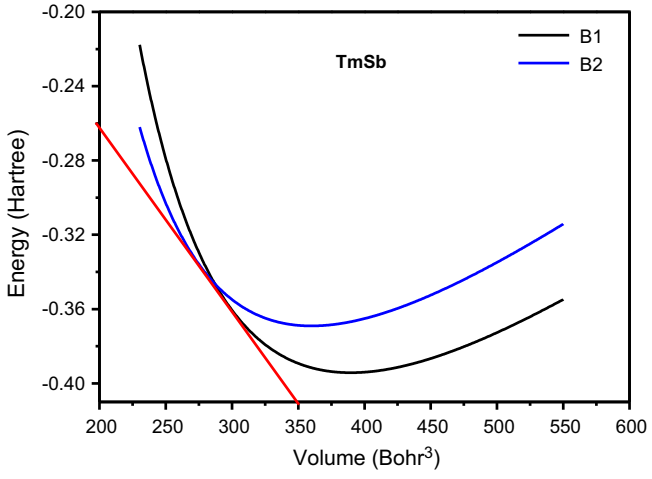

Fig. 1. Energy–volume curves for B1 and B2 structures of TmSb.

Table 1
Calculated lattice constant (a), bulk modulus (B), pressure derivative of bulk modulus (B'), phase transition pressure (P_t), and cohesive energy (E_{coh}) for B1 and B2 structure of TmSb.

Material	Reference	a (Å)	B (GPa)	B'	P_t (GPa)	E_{coh} (eV/atom)
TmSb (B1)	Present$^{(GGA_PBE)}$	6.1354	60.71	4.03	29.13$^{(from\ H-P)}$	5.24
	Present$^{(GGA_PBE)}$				29.38$^{(from\ tangent)}$	
	Expt.	6.1054[a]				
	Expt.	6.08[b]				
	Expt.		71.73[c]			
	Expt.				31[d]	
	Theo.		70.04[e]	5.86[e]	29.8[e]	
TmSb (B2)	Present$^{(GGA_PBE)}$	3.7643	61.59	3.90		3.92
	Expt.	3.46[d]				

[a] Ref. [25].
[b] Ref. [30].
[c] Ref. [29].
[d] Ref. [24].
[e] Ref. [31].

than those obtained by Shirotani et al. [24] and also very close to the other theoretical value of 29.8 GPa presented by Soni et al. [31](see Table 1).

The volume–pressure curves were plotted for B1 and B2 phase of this compound (see Fig. 2). As expected, the cell volume decreases with increasing pressure, and the discontinuity in volume takes place at the phase transition pressure.

The cohesive energy (E_{coh}) of a given phase is defined as the difference in the total energy of the constituent atoms at infinite separation and the total energy of that particular phase:

$$E_{coh}^{AB} = \left[E_{atom}^{A} + E_{atom}^{B} - E_{total}^{AB}\right] \quad (10)$$

where E_{total}^{AB} is the total energy of the TmSb at equilibrium lattice constant, E_{atom}^{A} and E_{atom}^{B} refer to the atomic energies of the pure constituents. The calculated E_{coh}, presented in Table 1, are estimated to be 5.24 and 3.92 eV/atom for B1 and B2 structures of TmSb, respectively. For B1 structure, E_{coh} value is very close to this found for HoSb as in our recent work [52].

3.2. Elastic and electronic properties

The elastic constants are important parameters which determine the response of the crystal to external forces and play an important role in determination of the strength, brittleness/ductility, and hardness of materials. Here, the "stress-strain" relations [53] were used to obtain the second-order elastic constants (C_{11}, C_{12}, and C_{44}), listed in Table 2, for both phases. The traditional mechanical stability conditions in cubic crystals on the elastic constants are known as $C_{11} - C_{12} > 0$, $C_{11} > 0$, $C_{44} > 0$, $C_{11} + 2C_{12} > 0$. For B1 structure, the calculated elastic constants in Table 2 obey these stability conditions and also obey the cubic stability condition: $C_{12} < B < C_{11}$. The calculted $C_{11} - C_{12}$ value is in good agreement with the experimental data of Mullen et al. [29] and other theoretical data of Soni et al. [31]. The deviation from experimental data [29] are found to be 6.1% for C_{11}, 35.25% for C_{12} and 5.15% for C_{44}. The presented C_{11}, C_{12}, and C_{44} are 5.6%, 29.4% lower, and 2.92% higher than the previous theoretical data [31], respectively. For B2 phase, $C_{11} - C_{12} > 0$, $C_{11} > 0$, $C_{44} < 0$, $C_{11} + 2C_{12} > 0$. It is noted that TmSb is mechanically unstable in B2 phase due to the negative C_{44} value and its elastic constants are not satisfy the cubic stability condition: $C_{12} < B < C_{11}$ (Here, $C_{12} > B$).

The difference between the two elastic constants C_{12} and C_{44} (i.e. $C_{12} - C_{44}$) is called as Cauchy pressure. Pettifor [54] and Johnson [55] have suggested that the angular character of atomic bonding in metals and compounds for cubic systems, which can be used to explain ductile/brittle properties of materials, may be described by the Cauchy pressure. It is typically positive for metallic non-directional bonding. On the other hand, it is negative for directional bonding with angular character. The more directional and less mobile of bonds represents by the larger negative values of Cauchy pressure. These correlations have, widely, been verified for some elements and compounds in the last decade [54,56–65]. In the present work, the negative Cauchy pressure is observed for B1 structure which shows the material will behave in brittle manner. The unusual behavior of the elastic constants of TmSb, most probably, stems from the electronic topological transitions. In general, it is believed that the negative Cauchy discrepancy is a consequence of the hybridization of the unstable 'f' band, and hybridization may be responsible for the decrease in Tm–Tm distance leading to a small value of the C_{12} (see Refs. [66] and [67] for other rare-earth compounds) i.e. the itinerant nature of the f-electrons in the rare-earth element Tm causes to the $C_{12} < C_{44}$ inequality.

We can also estimate the plastic properties of polycrystalline materials from the elastic properties based on the Pugh's criterions [68]. According to Pugh, materials having a B/G ratio greater than 1.75 are ductile whereas materials having a B/G ratio less than 1.75 are considered brittle. Here, for B1 structure the B/G is found to be 1.597. It is lower than 1.75 which also indicates that the material is expected to be brittle in nature.

To see the effect of pressure on the elastic constants, the pressure dependence behavior of the second-order elastic constants is also investigated up to 18 GPa (see Fig. 3) for B1 and B2 phases. From Fig. 3 (a) and (b), the $C_{11} > 0$, $C_{12} > 0$, and $C_{44} > 0$ for B1 phase whereas $C_{11} > 0$, $C_{12} > 0$, and $C_{44} < 0$ for B2 phase. While C_{12} and C_{44} decrease, C_{11} increases with increasing pressure for B1 phase. For B2 phase, C_{11} increases with pressures from 0 to 4 GPa and for $P > 4$ GPa it decreases with pressure. C_{12} increases with increasing pressure, C_{44} decreases with 0–10 GPa and for $P > 10$ GPa it

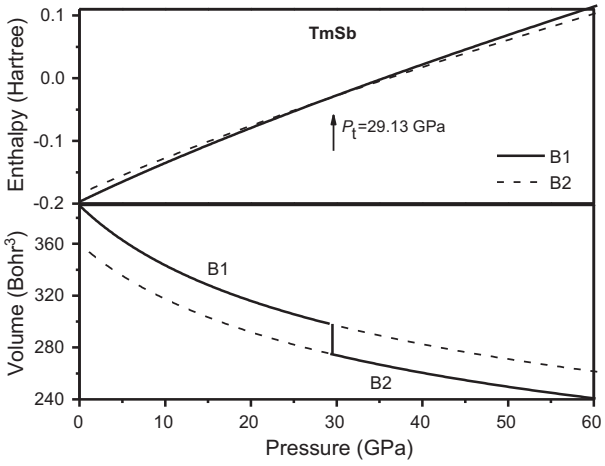

Fig. 2. Enthalpy–pressure and volume–pressure curves for B1 and B2 structures of TmSb.

Table 2
Elastic constants (in GPa) for TmSb in B1 and B2 structures.

Material	Reference	C_{11}	C_{12}	C_{44}	$C_{11} - C_{12}$
TmSb (B1)	Present	151.898	17.289	25.421	134.609
	Expt.	161.7[a]	26.7[a]	26.800[a]	135[a]
	Theo.	160.9[b]	24.5[b]	24.7[b]	136.4[b]
TmSb (B2)	Present	66.777	66.052	−33.986	0.725

[a] Ref. [29].
[b] Ref. [31].

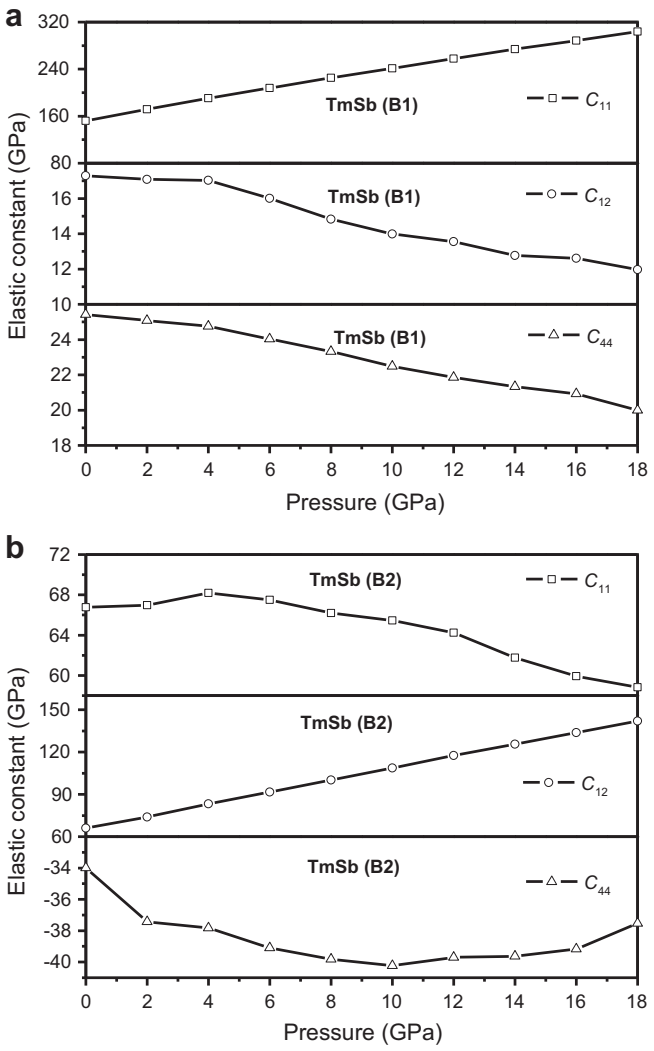

Fig. 3. The pressure dependent behavior of elastic constants for (a) B1 and (b) B2 structures of TmSb.

increases with P for the same phase. The B2 phase of this compound is elastically unstable with respect to shear distortion at all pressures. Therefore, C_{11} and C_{12} exhibit opposite behavior for B1 and B2 as in Fig. 3.

We also calculated the Zener anisotropy factor (A), Poisson's ratio (ν), and Young's modulus (E), which are frequently measured for polycrystalline materials when investigating their hardness. The Zener anisotropy factor, A, is calculated using the relation given as [69]

$$A = \frac{2C_{44}}{C_{11} - C_{12}}. \tag{11}$$

Poisson's ratio, ν, and Young's modulus, E, are calculated in terms of the computed data using the following relations [70]:

$$\nu = \frac{1}{2}\left[\frac{\left(B - \frac{2}{3}G\right)}{\left(B + \frac{1}{3}G\right)}\right], \tag{12}$$

and

$$E = \frac{9GB}{G + 3B}, \tag{13}$$

where $G = (G_V + G_R)/2$ is the isotropic shear modulus, G_V is Voigt's shear modulus corresponding to the upper bound of G values, and G_R is Reuss's shear modulus corresponding to the lower bound of G values; they can be written as: $G_V = (C_{11} - C_{12} + 3C_{44})/5$, and $5/G_R = 4/(C_{11} - C_{12}) + 3/C_{44}$.

The calculated Zener anisotropy factor, A, Poisson's ratio, ν, Young's modulus, E, and shear modulus, G (9.7% lower than the other theoretical data [31]), for TmSb are presented in Table 3 along with the previous theoretical data.

The Zener anisotropy factor, A, takes the value of 1 for a completely isotropic material. When A value is smaller or greater than unity, it is a measure of the degree of elastic anisotropy. The calculated A value for TmSb is smaller than 1 which indicates that this compound exhibits an elastically anisotropic character. It is in good agreement with the other theoretical value of Ref. [31].

Poisson's ratio, ν, is small ($\nu = 0.1$) for covalent materials, and it has a typical value of $\nu = 0.25$ for ionic materials [71]. In our case, the ν value for TmSb is equal to 0.241, i.e. a considerable ionic contribution in atomic bonding takes place for this phase. It is 85.4% higher than the theoretical value of 0.13 as in Ref. [31].

The Young's modulus, E, is defined as the ratio between stress and strain and used to provide a measure of the stiffness of the solids i.e. the material is stiffer for the larger value of E. The calculated E value is 94.342 GPa which is consistent with this found for HoSb as in our recent work [52] and 38.86% lower than the other theoretical value given in Ref. [31].

Although it is not our main purpose, the calculated electronic band structures and the related total density of sates (TDOS) for the B1 phase at 0 GPa are shown in Fig. 4. From this figure, it can be seen that there are some bands that not cross the Fermi level (the Fermi level (E_F) is set to zero of energy) indicating the nearly semimetallic behavior of B1-TmSb. The TDOS is compatible with the band structure results.

3.3. Thermodynamic properties

For B1 phase of TmSb, the thermal properties are determined in the temperature range 0–1000 K. The calculations based on the first principles methods demonstrate that the quasi-harmonic approximation provides a reasonable description of the dynamic properties of many bulk materials below the melting point [72–76]. The melting point of this compound is calculated to be (1450.717 ± 300.000) K. Therefore, for decreasing the probable influence of anharmonicity, the thermal properties are determined in the temperature range from 0 to 1000 K, where the quasi-harmonic model remains fully valid. The pressure effect is studied in the 0–18 GPa range which was chosen to be smaller than the transition pressure.

The dependence of normalized volume, V/V_0, on pressure (0–18 GPa) at different temperatures (0–1000 K) are investigated and illustrated for B1 structure in Fig. 5. It is obviously seen from

Table 3
The calculated Zener anisotropy factor (A), Poisson's ratio (ν), Young's modulus (E), shear modulus (G), and Debye temperature (Θ) for $T = 0$ K, $T = 200$ K at $P = 0$ GPa for TmSb in B1 structure.

Material	Reference	A	ν	E (GPa)	G (GPa)	Θ(K)
TmSb (B1)	Present$^{(\text{for T = 0 K})}$	0.377	0.241	94.342	38.010	230.88
	Present$^{(\text{for T = 200 K})}$					228.31
	Expt.					187[a]
	Expt. $^{(\text{for T = 200 K})}$					237[b]
	Theo.	0.36[c]	0.13[c]	154.3[c]	42.1[c]	236.9[c]

[a] Ref. [25].
[b] Ref. [29].
[c] Ref. [31].

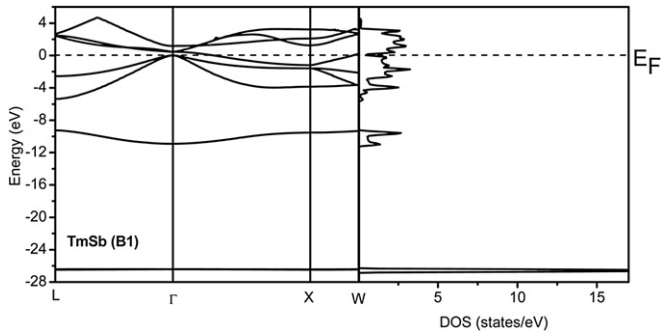

Fig. 4. Electronic band structure and total density of states of TmSb in B1 structure.

Fig. 5 that, the V/V_0 values decrease as the pressure increases at a given temperature. At the same pressure, the values of V/V_0 of higher temperature is less than that of lower temperature. We can say that, as temperature T increases, V/V_0–P curve becomes steeper which indicates that the compressibility of TmSb increases with increasing temperature.

The variations of bulk modulus, B, with temperatures and pressures are presented in Fig. 6 for B1 structure. For $T < 30$ K the B values keep constant. At higher temperatures, it exhibits rapid decrease with increasing temperature at a given pressure indicating rapid cell volume changes. It exhibits rapid increase as pressure increases at a given temperature. At the same pressure, the values of the bulk modulus B at $T > 0$ K are less than that at $T = 0$ K.

For B1 structure, the temperature dependence of the heat capacity at constant volume, C_V, at different pressures, presented in Fig. 7, follows the Debye Law. At low temperatures ($T < 250$ K), C_V tends to zero when the temperature vanishes and it increases rapidly with temperature at a given pressure. However, at high temperatures ($T > 250$ K), the anharmonic effect on C_V is suppressed, and C_V is very close to the Dulong-Petit limit as shown in Fig. 7.

Fig. 8 shows dependence of the predicted thermal expansion coefficient, α, on temperature for the B1 structure of TmSb. It is shown that, for a given pressure, at low temperature ($T < 250$ K), α rises quickly with temperature. Relatively at high temperatures ($T > 250$ K), it increases slowly with temperature at all pressures. We can say that, as the pressure increases, the increase of α with temperature becomes smaller. The thermal expansion coefficient has been reported as 10.8×10^{-6} K^{-1} by Abdusalyamova et al. [25]

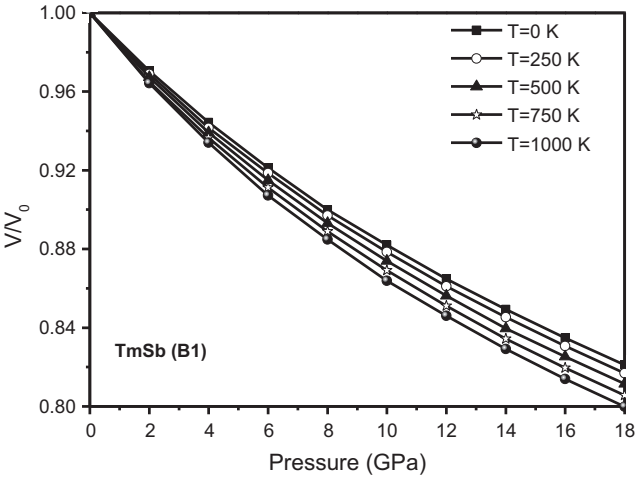

Fig. 5. Normalized volume–pressure curves for B1 phase of TmSb.

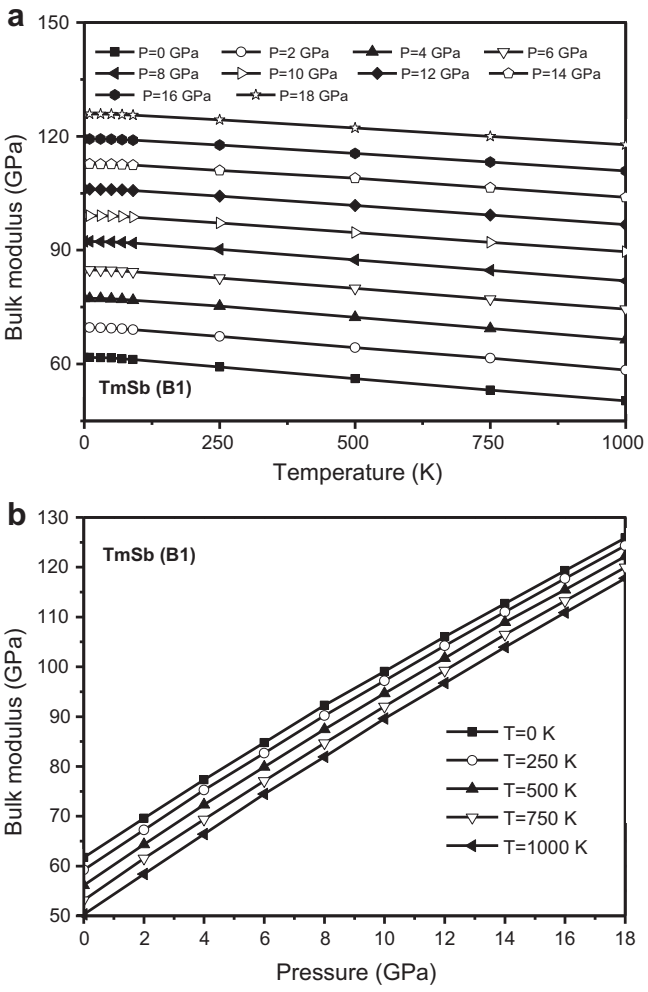

Fig. 6. The variations of bulk modulus with (a) temperature and (b) pressure for B1 structure of TmSb.

which is consistent with the presented α value at $P = 6$ GPa and $T = 50$ K (10.17×10^{-6}K^{-1}).

The Debye temperature (Θ), closely related to the elastic constants, specific heat, and melting temperature, was calculated

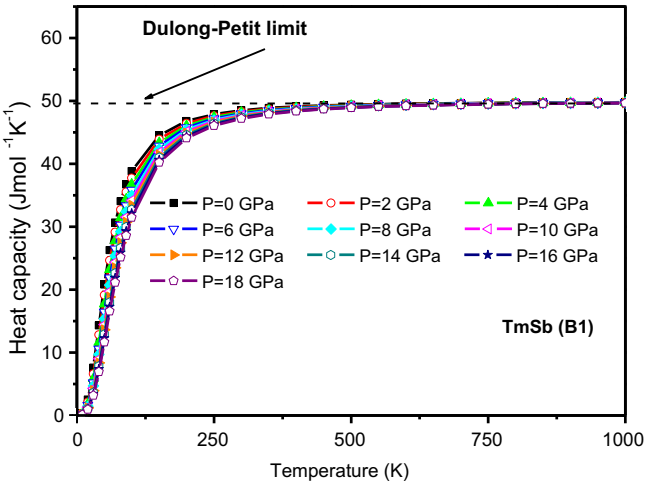

Fig. 7. The heat capacity of TmSb in B1 structure as a function of temperature at various pressures.

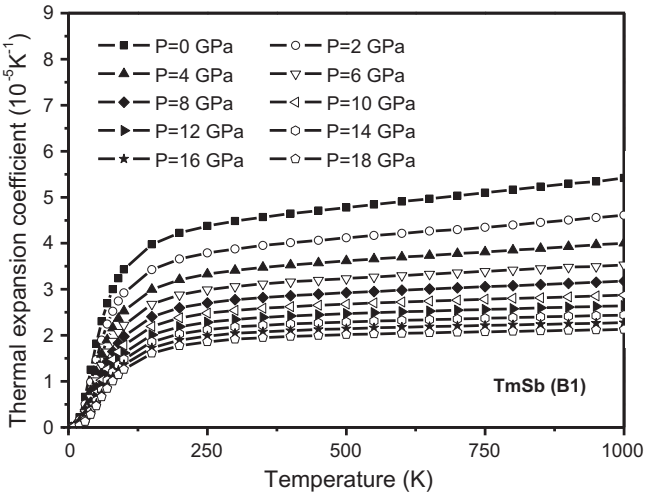

Fig. 8. The thermal expansion coefficient versus temperature at different pressures for TmSb in B1 structure.

for B1 structure in quasi-harmonic approximation. As shown in Fig. 9 (a), for $T < 30$ K the values of Θ are constant and for $T > 30$ K Θ values decrease with the temperature, but increase as pressure increases (see Fig. 9 (b)). At high pressures (from $P > 10$ GPa), when

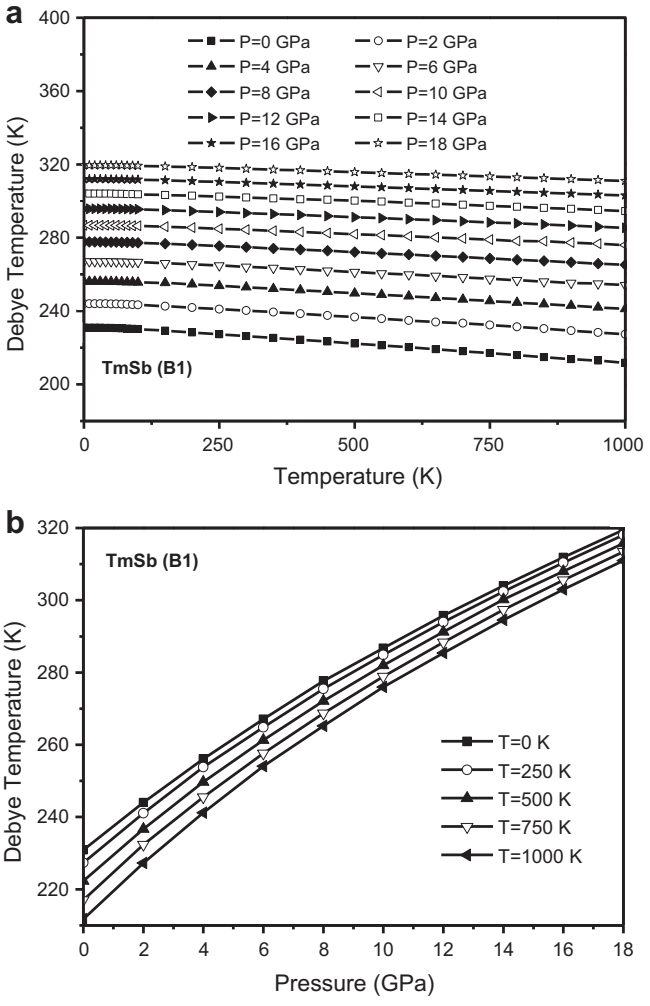

Fig. 9. The variations of Debye temperature with (a) temperature and (b) pressure for TmSb in B1 structure.

Table 4
The variations of calculated Grüneisen parameter (γ) with different temperature and pressure for B1 structure of TmSb.

Material: TmSb						
T (K)		0	250	500	750	1000
P (GPa)	Reference			γ		
0	Present	1.881	1.902	1.932	1.964	1.996
2	Present	1.805	1.822	1.847	1.873	1.903
4	Present	1.738	1.751	1.773	1.797	1.821
6	Present	1.680	1.692	1.710	1.730	1.749
8	Present	1.626	1.637	1.654	1.671	1.690
10	Present	1.582	1.591	1.605	1.620	1.635
12	Present	1.540	1.548	1.561	1.574	1.588
14	Present	1.503	1.510	1.520	1.533	1.545
16	Present	1.469	1.475	1.486	1.496	1.508
18	Present	1.438	1.443	1.453	1.463	1.473

the temperature is constant, the change in the Θ increases almost linearly with pressure. The Debye temperature of TmSb has been reported by Abdusalyamova et al. [25] and Mullen et al. [29]. At 200 K, the calculated value of Θ for B1 structure of TmSb, presented in Table 3, is 3.6% lower than the experimental data of the Ref. [29]. The presented Θ value at 0 K, is roughly 23.5% higher than that reported in Ref. [25]. It is 2.54% lower than the other theoretical data given in Ref. [31].

The Grüneisen parameter, γ, is a key quantity in this model which could describe the alteration in vibration of a crystal lattice based on the increase or decrease in volume as a result of temperature change [77]. For B1 structure, it is given in Table 4 for various temperatures and pressures. As can be seen, at constant pressure, the calculated γ slightly increases with temperature and in practice, one can think that it remains constant. It decreases rapidly with pressure for TmSb at a given temperature.

At different pressures, the temperature dependent behavior of entropy, S, for TmSb compound is presented in Fig. 10. The entropy increases with temperature but it decreases with the pressure. At high temperatures (for $T > 500$ K), the change in the S increases almost linearly with temperature.

3.4. Phonon properties

To better understand the dynamical behavior, we investigated the energy dispersion of phonons in this material for B1 structure. The phonon dispersion curves and one-phonon DOS

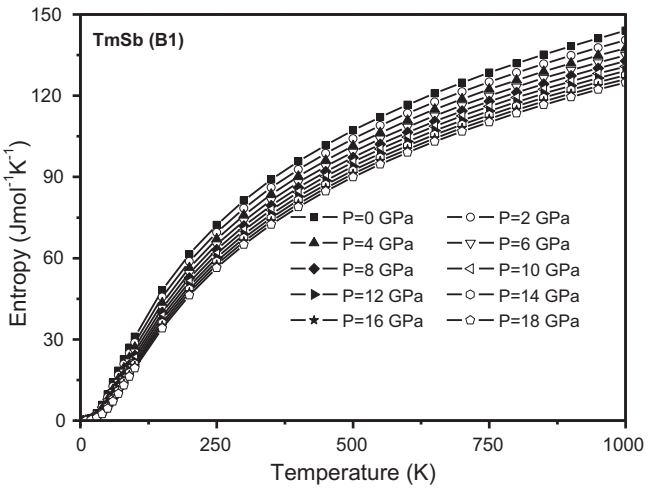

Fig. 10. The entropy of TmSb in B1 structure at various temperatures and pressures.

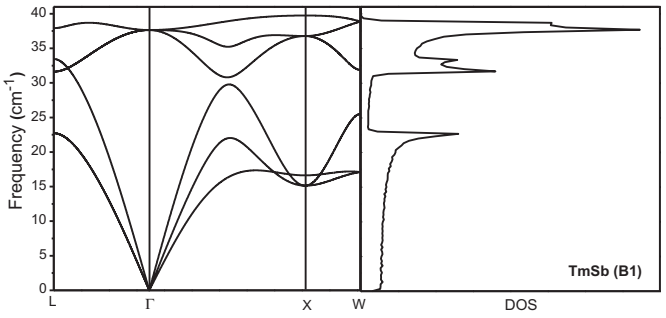

Fig. 11. Calculated phonon dispersion curves and one-phonon density of states for TmSb in B1 structure.

without LO/TO splitting of TmSb were calculated and plotted in Fig. 11. Here, a small gap between the acoustic and optical branches is only observed in the Γ X direction. The B1 phase is stable dynamically because the negative frequencies (soft modes) are not observed for any wave vector. There are no experimental or other theoretical data for the comparison with our calculated results.

4. Summary and conclusion

In conclusion, we studied structural, elastic, electronic, thermodynamic, and phonon properties of TmSb compound which crystallizes in B1 structure by using ab-initio calculations. The optimized lattice parameters (a), bulk modulus (B), pressure derivative of bulk modulus (B'), the cohesive energies (E_{coh}), and second-order elastic constants (C_{ij}) are presented for B1 and B2 structures. Except E_{coh} values, all the structural parameters were compared with the available previous results. The E_{coh} values were obtained and reported here for the first time, to our knowledge. The calculated pressure at which these compounds undergoes a structural phase transition from B1 to B2 phase agrees well with previous experimental and theoretical data. The elastic properties such as Zener anisotropy factor (A), Poisson's ratio (ν), Young's modulus (E), shear modulus (G) were calculated for B1 which are in good agreement with available other theoretical values. The calculated elastic constants satisfy the traditional mechanical stability conditions except C_{44} for B2 phase. For B1 structure, we analyzed the behavior of relative volume and bulk modulus of TmSb for a pressure range of 0–18 GPa up to 1000 K. It is found that, while the normalized volume decreases with increasing pressure, the bulk modulus, B, increases with the increase of pressure. The temperature dependences of heat capacity, C_V, and thermal expansion coefficient, α, at various pressures were investigated. Finally, Debye temperature, Θ, Grüneisen parameter, γ, and entropy, S, were calculated at different temperatures and pressures. The electronic band structure, total density of states, phonon dispersion curves and one-phonon DOS for B1 were calculated and depicted in Figs. 4 and 11, respectively.

Acknowledgements

This work is supported by Gazi University Research- Project Unit under Project No: 05/2009-55.

References

[1] C.J.M. Rooymans, Structural Investigations on Some Oxides and Other Chalcogenides at Normal and Very High Pressures (Philips Research Reports). Philips, Eindhoven, 1968.
[2] A. Chatterjee, A.K. Singh, A. Jayaraman, Phys. Rev. B 6 (1972) 2285.
[3] A. Jayaraman, A.K. Singh, A. Chatterjee, S. Usha Devi, Phys. Rev. B 9 (1974) 2513.
[4] V.V. Shchennikov, N.N. Stepanov, I.A. Smirnov, A.V. Golubkov, Sov. Phys.-Solid State 30 (1988) 1785.
[5] U. Benedict, W.B. Holzapfel, in: K.A. Gschneidner, L. Eyring, G.H. Lander, G.R. Choppin (Eds.), Handbook on the Physics and Chemistry of Rare Earths, North-Holland, Amsterdam, 1993.
[6] V.A. Sidorov, N.N. Stepanov, L.G. Khvostantsev, O.B. Tsiok, A.V. Golubkov, V.S. Oskotski, I.A. Smirnov, Semicond. Sci. Technol. 4 (1989) 286.
[7] O.B. Tsiok, V.A. Sidorov, V.V. Bredikhin, L.G. Khvostantsev, Solid State Commun. 79 (1991) 227.
[8] T. Le. Bihan, S. Darracq, S. Heathman, U. Benedict, K. Mattenberger, O. Vogt, J. Alloy. Compd. 226 (1995) 143.
[9] J.M. Leger, R. Epain, J. Loriers, D. Ravot, J. Rossat-Mignod, Phys. Rev. B l (1983) 7125.
[10] J.M. Leger, D. Ravot, J. Rossat-Mignod, J. Phys. C Solid State Phys. 17 (1984) 4935.
[11] N. Mori, Y. Okayama, H. Takahashi, Y. Haga, T. Suzuki, Physica B 186–188 (1993) 444.
[12] U. Benedict, J. Alloy. Compd. 223 (1995) 216.
[13] I. Shirotani, K. Yamanashi, J. Hayashi, Y. Tanaka, N. Ishimatsu, O. Shimomura, T. Kikegawa, J. Phys. Condens. Matter 13 (2001) 1939.
[14] I. Shirotani, K. Yamanashi, J. Hayashi, N. Ishimatsu, O. Shimomura, T. Kikegawa, Solid State Commun. 127 (2003) 573.
[15] C. Çoban, K. Çolakoğlu, Y. ÖÇiftçi, Mater. Chem. Phys. 125 (2011) 887.
[16] A. Svane, G. Santi, Z. Szotek, W.M. Temmerman, P. Strange, M. Horne, G. Vaitheeswaran, V. Kanchana, L. Petit, H. Winter, Phys. Status Solidi b 241 (2004) 3185.
[17] D. Singh, M. Rajagopalan, A.K. Bandyopadhyay, Solid State Commun. 112 (1999) 39.
[18] D. Singh, M. Rajagopalan, M. Husain, A.K. Bandyopadhyay, Solid State Commun. 115 (2000) 323.
[19] D. Singh, V. Srivastava, M. Rajagopalan, M. Husain, A.K. Bandyopadhyay, Phys. Rev. B 64 (2001) 115110.
[20] V.N. Antonov, B.N. Harmon, A.N. Yaresko, Phys. Rev. B 66 (2002) 165208.
[21] G. Vaitheeswaran, V. Kanchana, M. Rajagopalan, J. Alloy. Compd. 336 (2002) 46.
[22] P. Pandit, V. Srivastava, M. Rajagopalan, S.P. Sanyal, Physica B 403 (2008) 4333.
[23] C.G. Duan, R.F. Sabirianov, W.N. Mei, P.A. Dowben, S.S. Jaswal, E.Y. Tsymbal, J. Phys. Condens. Matter 19 (2007) 315220.
[24] I. Shirotani, J. Hayashi, K. Yamanashi, N. Ishimatsu, O. Shimomura, T. Kikegawa, Phys. Rev. B 64 (2001) 132101-1.
[25] M.N. Abdusalyamova, O.I. Rakhmatov, High Temperature 40 (2002) 636 Translated from Teplofizika Vysokikh Temperatur 40 (2002) 683.
[26] H.R. Ott, B. Lüthi, Phys. Rev. Lett. 36 (11) (1976) 600.
[27] Y.H. Wong, Phys. Rev. B 17 (10) (1978) 3899.
[28] B.R. Cooper, O. Vogt, Phys. Rev. B 1 (3) (1970).
[29] M.E. Mullen, B. Lüthi, P.S. Wang, E. Bucher, L.D. Longinotti, J.P. Maita, H.R. Ott, Phys. Rev. B 10 (1974) 186.
[30] F. Hulliger, in: K.A. Gschneidner, L. Eyring (Eds.), Handbook on the Physics and Chemistry of Rare Earths, vol. 4, North-Holland, Amsterdam, 1979 p. 153.
[31] P. Soni, G. Pagare, S.P. Sanyal, J. Phys. Chem. Solids 71 (2010) 1491.
[32] G. Kresse, J. Hafner, Phys. Rev. B 47 (1993) 558.
[33] G. Kresse, J. Hafner, J. Phys. Condens. Matter 6 (1994) 8245.
[34] G. Kresse, J. Hafner, Phys. Rev. B 49 (1994) 14251.
[35] G. Kresse, J. Furthmüller, Comput. Mater. Sci. 6 (1996) 15.
[36] G. Kresse, J. Furthmüller, Phys. Rev. B 54 (1996) 11169.
[37] T. Demuth, J. Hafner, L. Benco, H. Toulhoat, J. Phys. Chem. B 104 (2000) 4593.
[38] J.P. Perdew, K. Burke, M. Ernzerhof, Phys. Rev. Lett. 77 (1996) 3865.
[39] P.E. Blöchl, Phys. Rev. B 50 (1994) 17953.
[40] H.J. Monkhorst, J.D. Pack, Phys. Rev. B 13 (1976) 5188.
[41] M.A. Blanco, E. Francisco, V. Luaña, Comput. Phys. Commun. 158 (2004) 57.
[42] A.A. Maradudin, E.W. Montroll, G.H. Weiss, I.P. Ipatova, Theory of Lattice Dynamics in the Harmonic Approximation. Academic Press, New York, 1971.
[43] M.A. Blanco, PhD thesis, Universidad de Oviedo, 1997, URL http://web.uniovi.es/qcg/mab/tesis.html.
[44] M.A. Blanco, A. Martín Pendás, E. Francisco, J.M. Recio, R. Franco, J. Mol. Struct. (Theochem) 368 (1996) 245.
[45] E. Francisco, J.M. Recio, M.A. Blanco, A. Martín Pendás, J. Phys. Chem. 102 (1998) 1595.
[46] E. Francisco, M.A. Blanco, G. Sanjurjo, Phys. Rev. B 63 (2001) 094107.
[47] M. Flórez, J.M. Recio, E. Francisco, M.A. Blanco, A. Martín Pendás, Phys. Rev. B 66 (2002) 144112.
[48] http://chianti.geol.ucl.ac.uk/~dario/ (1998).
[49] D. Alfè, G.D. Price, M.J. Gillan, Phys. Rev. B 64 (2001) 045123-1.
[50] G. Kresse, J. Furthmüller, J. Hafner, Europhys. Lett. 32 (1995) 729.
[51] F.D. Murnaghan, Proc. Natl. Acad. Sci. USA 30 (1944) 244.
[52] C. Çoban, K. Çolakoğlu, Y. Ö Çiftçi, Phys. B Condens. Matter 405 (2010) 3977.
[53] O.H. Nielsen, R.M. Martin, Phys. Rev. Lett. 50 (1983) 697.
[54] D.G. Pettifor, Mater. Sci. Technol. 8 (1992) 345.
[55] R.A. Johnson, Phys. Rev. B 37 (1988) 3924.
[56] R.B. Karki, J.L. Stixrude, S.J. Clark, M.C. Warren, G.J. Ackland, J. Crain, Am. Mineral. 82 (1997) 51.

[57] D. Nguyen-Manh, D.G. Pettifor, S. Snam, V. Vitek, Mater. Res. Soc. 491 (1998) 353.
[58] A. Zahoui, B. Bcuhfs, P. Ruterana, Mater. Chem. Phys. 91 (2005) 108.
[59] M.J. Mehl, R.J. Hemley, L.L. Boyer, Phys. Rev. B 33 (1986) 8685.
[60] K. Chen, L.R. Zhao, J. Appl. Phys. 93 (2003) 2414.
[61] H. Boppart, A. Treindl, P. Wachter, S. Roth, Solid State Commun. 35 (1980) 483.
[62] R. Pasianot, D. Farkas, E.J. Savino, Phys. Rev. B 43 (1991) 6952.
[63] I.D. Bleskov, E.A. Smirnova, Yu. Kh. Vekilov, P.A. Korzhavyl, B. Johansson, M. Katsnelson, L. Vitos, I.A. Abrikosov, E.I. Isaev, App. Phys. Lett. 94 (2009) 161901.
[64] M.J. Cawkwell, D. Nyugen-Manh, V. Vitek, D.G. Pettifor, Mat. Res. Soc. Symp. Proc. 779 (2003) W5.5.1.
[65] M. Aoki, T. Kurokawa, J. Phys. Condens. Matter 19 (2007) 236228.
[66] D.C. Gupta, S. Kulshrestha, J. Phys. Condens. Matter 21 (2009) 436011.
[67] D.C. Gupta, A.K. Baraiya, J. Alloy. Compd. 499 (2010) 90.
[68] S.F. Pugh, Philos. Mag 45 (1954) 823.
[69] C. Zener, Elasticity and Anelasticity in Metals. University of Chicago Press, Chicago, 1948.
[70] B. Mayer, H. Anton, E. Bott, M. Methfessel, J. Sticht, J. Haris, P.C. Schmidt, Intermetallics 11 (2003) 23.
[71] V.V. Bannikov, I.R. Shein, A.L. Ivanovskii, Phys. Status Solidi (RRL) 1 (2007) 89.
[72] S. Biernacki, M. Scheffler, Phys. Rev. Lett. 63 (1989) 290.
[73] A. Fleszar, X. Gonze, Phys. Rev. Lett. 64 (1990) 2961.
[74] P. Pavone, K. Karch, O. Schutt, W. Windl, D. Strauch, P. Giannozzi, S. Baroni, Phys. Rev. B 48 (1993) 3156.
[75] P. Pavone, S. Baroni, S. De Gironcoli, Phys. Rev. B 57 (1998) 10421.
[76] A.A. Quong, A.Y. Liu, Phys. Rev. B 56 (1997) 7767.
[77] J.-J. Tan, Y. Cheng, W.-J. Zhu, Q.-Q. Gou, Commun. Theor. Phys. 50 (1) (2008) 220.